Proc. Natl. Acad. Sci. USA
Vol. 86, pp. 2473–2477, April 1989
Neurobiology

Sodium channels in dendrites of rat cortical pyramidal neurons

(dendritic spikes/sodium currents/neuronal integration)

JOHN R. HUGUENARD, OWEN P. HAMILL*, AND DAVID A. PRINCE

Department of Neurology, Stanford University Medical Center, Stanford, CA 94305

Communicated by Dominick P. Purpura, December 20, 1988 (received for review October 14, 1988)

ABSTRACT **The voltage-dependent properties that have been directly demonstrated in Purkinje cell and hippocampal pyramidal cell dendrites play an important role in the integrative capacities of these neurons. By contrast, the properties of neocortical pyramidal cell dendritic membranes have been more difficult to assess. Active dendritic conductances near sites of synaptic input would have an important effect on the input–output characteristics of these neurons. In the experiments reported here, we obtained direct evidence for the existence of voltage-dependent Na^+ channels on the dendrites of neocortical neurons by using cell-attached patch and whole cell recordings from acutely isolated rat neocortical pyramidal cells. The qualitative and quantitative properties of dendritic and somatic currents were indistinguishable. Insofar as Na^+ currents are concerned, the soma and primary apical dendrite can be considered as one relatively uniform compartment. Similar dendritic Na^+ currents on dendrites in mature neurons would play an important role in determining the integrative properties of these cortical units.**

Contrary to earlier concepts (1), recent data suggest that dendritic membranes of neurons in the mammalian cerebellum (2) and hippocampus (3–5) possess voltage-dependent conductances that lead to spike generation and play an important role in the integrative activities of these cells (2, 6). Evidence of dendritic spike generation in cortical pyramidal neurons is less complete. It has been proposed that low-amplitude, short-duration spikes seen in recordings from these cells in mature and immature neocortex are generated by voltage-dependent dendritic processes (7, 8), although other explanations are possible (9). However, because of the fine caliber of neocortical pyramidal cell dendrites and the absence of a discrete dendritic layer, the anatomically confirmed, high-quality intradendritic recordings necessary to further evaluate membrane electroresponsiveness have been largely unavailable (10). We have used acutely isolated cortical neurons (11, 12) and patch clamp techniques (13) to obtain direct evidence for the presence of voltage-dependent Na^+ channels on the dendrites of rat neocortical pyramidal cells and have determined that, within the age range studied [postnatal days 2–6 (P2–P6)], the density and voltage dependence of Na^+ channels on somatic and primary dendritic membrane are comparable.

MATERIALS AND METHODS

Neocortical pyramidal cells were isolated by using a combination of enzymatic and mechanical techniques (14) based on the methods of Wong and coworkers (11, 12). Rat pups aged P2–P6 were anesthetized by cooling and then were decapitated. Brains were quickly removed, and 600-μm coronal slices containing sensorimotor cortex were cut on a vibratome (Lancer). Pieces of neocortex (1 mm^2) were trimmed, incubated in a solution containing trypsin at 1 mg/ml, and then mechanically dispersed by trituration with fire-polished Pasteur pipettes.

Pyramidal neurons in isolation (e.g., Figs. 1*A*, 2*C*, and 3*A*) were identified by their morphological features, which included large (diameter >15 μm) somata and one major apical dendrite measuring up to 100 μm in length (14). In other experiments we found that these characteristics correlated with a lack of positive immunocytochemical staining for glutamic acid decarboxylase, the synthetic enzyme for γ-aminobutyric acid, the major neurotransmitter found in inhibitory interneurons.

Whole cell Na^+ currents were isolated by recording from neurons bathed in an extracellular solution containing 145 mM NaCl, 3 mM KCl, 1 mM $MgCl_2$, 1 mM $CaCl_2$, 0.5 mM $CdCl_2$, and 10 mM Hepes, adjusted to pH 7.3 with NaOH, and using patch pipettes filled with a solution containing 120 mM CsF, 10 mM tetraethylammonium chloride, 5 mM NaCl, 1 mM $MgCl_2$, 1 mM $CaCl_2$, 11 mM EGTA, and 10 mM Hepes, adjusted to pH 7.3 with CsOH. Under these conditions, all residual active current was tetrodotoxin (TTX) sensitive (e.g., note TTX trace in Fig. 2*A*, where only uncompensated capacitative and leak currents remain), indicating that Na^+ currents were, in fact, isolated. For cell-attached patch recordings, the same extracellular solution was used, and the pipette solution consisted of 145 mM sodium aspartate, 2 mM 4-aminopyridine, 1 mM $MgCl_2$, 0.5 mM $CdCl_2$, and 10 mM Hepes at pH 7.3. Na^+ channel currents were identified by their voltage dependence of activation and inactivation, which was essentially the same as for whole cell Na^+ currents, as identified by TTX sensitivity. Patch pipettes (1–4 MΩ) were pulled from thin-walled borosilicate glass (WPI Instruments, Waltham, MA, no. TW-150), and current recordings were obtained with a List Electronics (Darmstadt, F.R.G.) EPC-7 patch clamp amplifier. All experiments were performed at room temperature (22–24°C).

We used two strategies to record dendritic Na^+ currents. In the first, whole cell recordings were employed, and dendritic currents were isolated by differential microperfusion in which Na^+ currents were evoked in one part of the cell perfused with a Na^+-containing solution and blocked in other cell regions with a 0-Na^+ solution. Two "puffer" pipettes were positioned near a pyramidal neuron, and the solutions were ejected from the pipettes by low-pressure (10–50 kPa) application of N_2 gas. The regions of influence of the two puffers were visualized by including different common food dyes (red or blue) in each solution. The boundary between the puffer solutions could be detected through the microscope (Fig. 1*A*), and the sharpness of this interface was verified in control experiments by using two test solutions with different Cl^- activities and determining the spatial gradient (which was always <15 μm) by measuring the liquid junction potential

The publication costs of this article were defrayed in part by page charge payment. This article must therefore be hereby marked "*advertisement*" in accordance with 18 U.S.C. §1734 solely to indicate this fact.

Abbreviations: TTX, tetrodotoxin; P*x*, postnatal day *x*.

*Present address: Department of Neurobiology and Behavior, Seeley G. Mudd Hall, Cornell University, Ithaca, NY 14853.

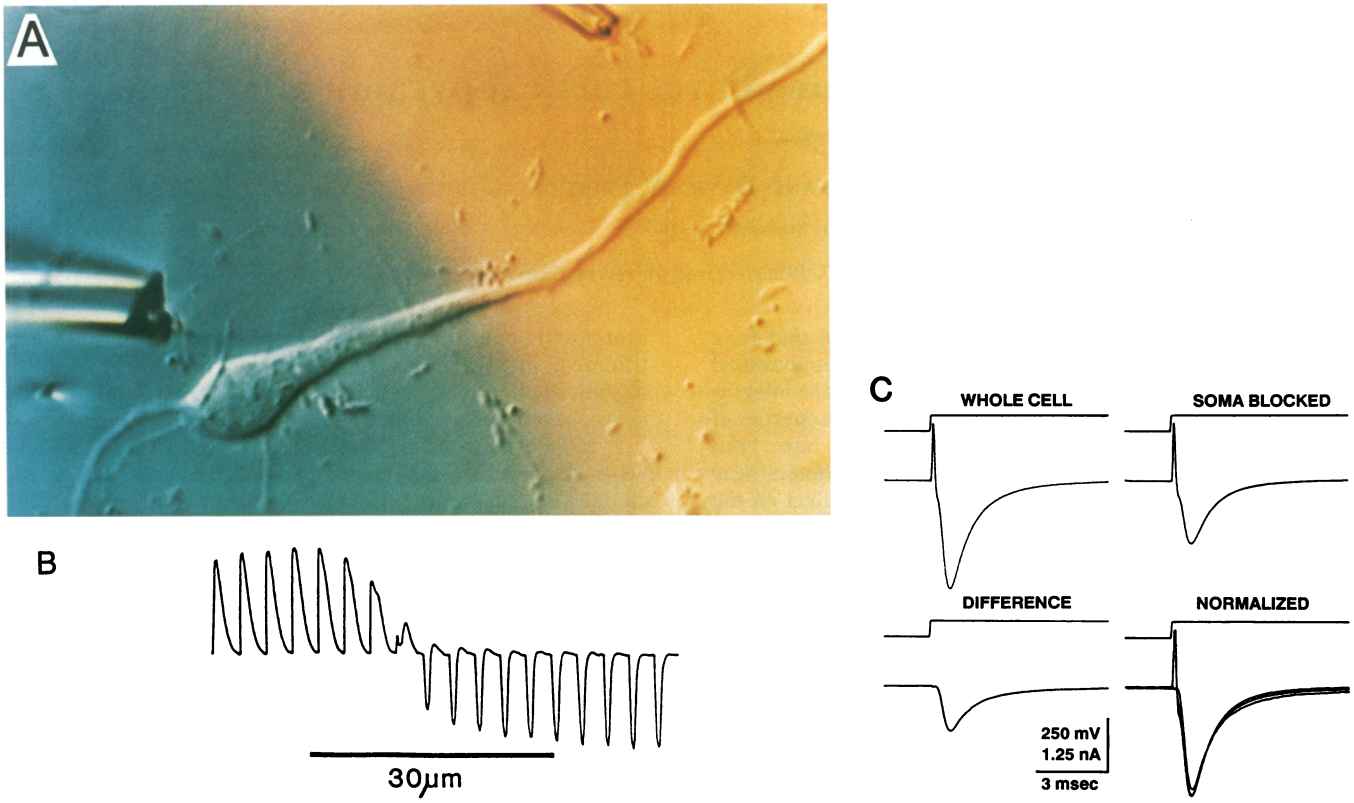

FIG. 1. (*A*) Differential microperfusion arranged so that extracellular Na^+ was available to only restricted portions of this P4 neocortical neuron. The orange-colored solution contained normal [Na^+], and the blue-colored solution contained equimolar Cs^+ substituted for Na^+. The plane of the boundary layer could be adjusted by moving either one or both of the perfusion pipettes. (*B*) The extent of the boundary layer of the differential perfusion is shown. Solutions with two different Cl^- concentrations were periodically ejected from two microperfusion pipettes while a patch electrode was advanced steadily across the field. The different junction potentials of the two Cl^- solutions caused inward or outward currents to be recorded with the patch clamp amplifier. The boundary layer always measured less than 15 μm. (*C*) Whole cell, Na^+ current obtained by perfusing the entire cell with Na^+ (Cs^+ pipette off); Soma blocked, dendritic Na^+ current obtained when the soma was blocked by Cs^+ solution; Difference, somatic Na^+ current obtained by subtracting dendritic current from whole cell current; Normalized, when the currents were normalized to peak current and superimposed, the time course of current activation and inactivation was similar for dendritic and somatic regions. Holding potential, −100 mV; command potential, −30 mV.

with a roving patch pipette (Fig. 1*B*). In control experiments, dye-containing solutions themselves had no effect on whole cell Na^+ currents, and the results of differential perfusion experiments were not affected by reversing the dye colors between the Na^+ current-enabling and -blocking solutions.

Dendrite diameters and lengths and somatic diameters were measured from photomicrographs of neurons taken during microperfusion experiments (Fig. 1*A*). Membrane surface areas were determined by assuming geometrical cell models in which dendrites were cylindrical and somata were spherical. We determined the regional density of Na^+ channels per square micrometer of cell membrane by dividing isolated dendritic or somatic Na^+ current obtained during differential perfusion by the area of the membrane that was perfused with Na^+-containing solution.

In a second set of experiments, we utilized the cell-attached configuration of the patch clamp (13) to directly obtain isolated recordings of dendritic versus somatic Na^+ channel activity in a given neuron. It was possible to record from up to four locations on the same neuron in some cases.

RESULTS

When whole cell current recordings were obtained with somatic electrodes containing CsF, graded inward currents with expected activation and inactivation kinetics could be evoked by a family of depolarizing voltage commands. Smooth current–voltage and activation curves and a voltage-dependent latency to peak current amplitude provided evidence that the neuron was under good space clamp control (14). These presumed Na^+ currents were blocked by perfusion of TTX (1 μM) or by perfusion with solutions in which choline was substituted for Na^+ (14).

Once stable whole cell Na^+ currents were obtained, we assessed the contributions of somatic versus dendritic membrane to the total Na^+ current by selectively perfusing different portions of the neuron as described above (Fig. 1*A*). When the bath solution contained choline or Cs^+ substituted for Na^+, no inward currents could be evoked. Focal application of a Na^+-containing solution from a puffer electrode directed either at the apical dendrite or soma, while the other site was being "protected" by perfusion from a puffer containing 0-Na^+, led to the development of an inward current with lower peak amplitude than the current obtained when the whole neuron was perfused with Na^+-containing solution (Fig. 1*C*). It was possible to approximate contributions from apical dendritic versus basal dendritic-somatic membranes by reversing the positions of the perfusion pipettes or by subtracting Na^+ currents obtained by perfusion of either site from the whole cell Na^+ current (Fig. 1*C*). Drawings of the cells used in differential perfusion experiments are shown in Fig. 2*C*, together with the perfusion boundaries (dotted lines). The results of these experiments indicated that portions of the apical dendritic membrane made a substantial contribution to the whole cell Na^+ conductance in isolated neurons. The relative density of Na^+ currents in proximal (soma-basilar dendritic) and distal

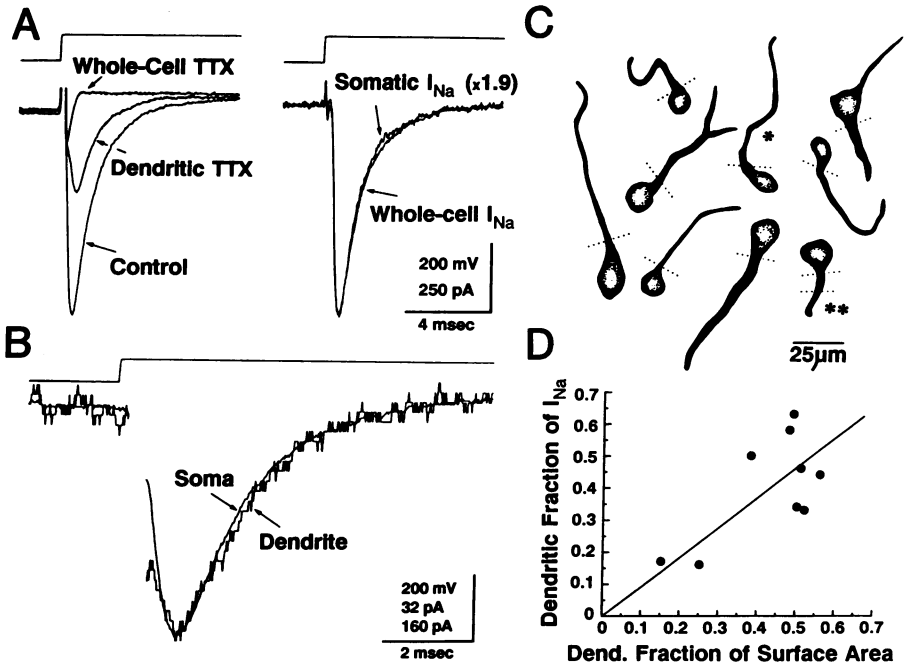

FIG. 2. (*A* and *B*) Direct comparisons of the time course of Na^+ current in different regions with leak and capacitative artifacts eliminated. When normalized to peak amplitude, Na^+ currents exactly overlap, indicating a uniform distribution of Na^+ channel types across neocortical pyramidal cell membranes. The stimulus protocol was a depolarization to −30 mV from a holding potential of −100 mV. (*A*) Leak and capacitative currents determined by applying command steps to the cell in TTX (1 μM)-containing solution. Somatic Na^+ currents (dendritic TTX) and whole cell (control) currents were then corrected by subtracting the currents obtained with whole cell TTX. (*B*) Scaled hyperpolarizing pulses were used for leak subtraction (15) while either the somatic or dendritic currents were isolated in low (10 mM) extracellular Na^+. The dendritic current is about 20% of the amplitude of the somatic current, whereas the time course of the Na^+ current is exactly the same for the two traces. During this experiment, the position of the two perfusion pipettes were reversed so that opposite parts of the neuron could be activated. (*C*) Outline drawings of cells used in differential perfusion experiments. The dotted lines indicate boundary planes of the differential perfusion. The neuron marked with the single asterisk was used in *A*, whereas that with the double asterisk was used in *B*. (*D*) Total and dendritic membrane areas were calculated to determine the fractional dendritic area. These values were compared to the fractional dendritic Na^+ current determined from differential perfusion. Linear regression of the results is shown as the solid line [slope = 0.93 ± 0.092 (mean ± SEM), r = 0.67].

(apical dendritic) membranes was similar. Regression analysis showed that there was a significant correlation between area and Na^+ current (Fig. 2*D* and Table 1). Several different selective perfusion strategies were used (see Table 1 legend), and each gave similar results.

By using the data obtained from differential perfusion experiments, it was also possible to determine whether there were significant differences between the properties of Na^+ currents on somatic and dendritic membranes. This was done by comparing current–voltage curves from the two sites in terms of their voltage dependence of activation (data not shown) and also by comparing single inward current traces for possible differences in kinetics of activation and inactivation (Fig. 2 *A* and *B*). In each case, no significant differences in these parameters were found between somatic and dendritic membranes.

Table 1. Dendritic Na^+ current versus dendritic surface area

Cell no.	Surface area, μm²		% dendritic area	% dendritic I_{Na}	Selective perfusion treatment*
	Somatic	Dendritic			
14.2714	340	373	52	33	Cs^+ soma
14.3166	429	391	48	58	Cs^+ soma
14.3691	432	420	49	63	Na^+ dendrite
15.3492	829	283	25	16	TTX soma
15.0003	389	393	50	34	Cs^+ dendrite
15.3331	765	789	51	46	TTX dendrite
29.1982	658	112	15	17	Na^+ soma or dendrite
15.2501	596	750	56	44	TTX soma
14.3003	759	457	38	50	Cs^+ dendrite

Surface areas were calculated as in Fig. 2. Where Na^+ current blocking agents were applied to soma, dendritic currents were obtained by subtracting somatic current from whole cell current and contrariwise when blocking agents were applied to dendrites.
*TTX, 1 μM TTX in blocking puffer; Cs^+, equimolar Cs^+ substituted for Na^+ in blocking puffer; Na^+, bath Na^+ replaced with Cs^+ and 10 mM Na^+ in enabling puffer; soma, dendrite, or soma or dendrite, enabling or blocking agent applied to indicated area.

In a second series of experiments, we took advantage of the cell-attached patch configuration of the patch clamp technique to directly compare Na^+ channel activity on somatic and dendritic membranes. This approach was possible because the apical dendrite often had a diameter of up to 4–5 μm for the first 50–100 μm from the soma-apical dendritic junction in neurons from younger animals (P2–P6). Electrodes with comparable tip sizes (resistance *ca.* 4 MΩ) were used so that patch areas at different sites would be approximately equivalent. Fig. 3 shows results from one neuron in which activities from four cell-attached patches were recorded sequentially (1-2-3-4) with separate patch electrodes. Fig. 3*B*, location 1 shows Na^+ channel currents (single traces and the ensemble average) activated by voltage commands in somatic patch, and Fig. 3*B*, location 2 shows comparable recordings from a dendritic patch about 80 μm away (see locations 1 and 2 in Fig. 3*A*). Fig. 3*B*, locations 3 and 4 show recordings from two additional sites [located at the junction of soma and apical dendrite (location 3 in Fig. 3 *A* and *B*) and further distal on the dendrite (location 4 in Fig. 3 *A* and *B*)] from the same neuron. Note that although there was Na^+ channel activity at each location, the density of channels was not precisely equivalent at all locations. For example, the dendritic location in Fig. 3*A*, location 4 had an unusually high level of Na^+ current; this would be indicative of a "hot spot"

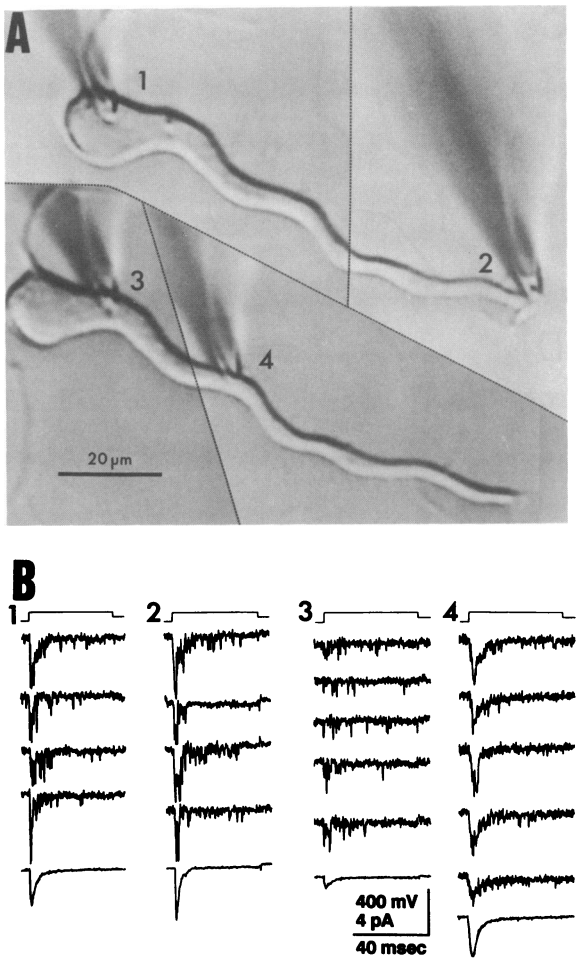

FIG. 3. Single-channel Na^+ currents recorded from cell-attached patches at multiple sites in a P5 neocortical pyramidal neuron. (*A*) Montage of placements (locations 1–4) of several cell-attached patch recording pipettes on the same pyramidal neuron. (*B*) Single-channel recordings obtained from the sites indicated in *A*. Depolarizations of 100 mV were applied from a holding potential 80 mV hyperpolarized from rest. The command potential in this case is expected to be near −30 mV. The records obtained in each column are from the locations labeled 1–4 in the photomicrograph in *A*. Representative traces (upper four sweeps) and the ensemble average of 50 consecutive traces (bottom sweep) are shown for each location. Calibration in *B* applies for locations 1–3, and the current calibration for location 4 is 8 pA. Current recordings were filtered at 2 kHz, and individual traces have been leak subtracted.

(16, 17). All recordings showed transient (about 1 msec), low-amplitude (1.5–2 pA) inward openings that were activated in a similar pattern by each voltage command at a given site (compare sequential sweeps in each vertical column of Fig. 3*B*). Comparable results were obtained from 24 somatic and 11 dendritic sites, including four cases in which 2 or 3 different sites on the same neuron were recorded. In other experiments ($n = 5$; data not shown), neurons were bathed in an isotonic potassium aspartate/low Ca^{2+} solution to bring the resting membrane potential to 0 (18), and the voltage dependence of activation of Na^+ channels was compared and shown to be the same for both dendritic and somatic sites.

Although it has been difficult to obtain recordings from neocortical neurons of older rats, we have been successful in confirming these results with cell-attached patch recordings in the somata and dendrites in neocortical pyramidal neurons from young (P3–P7) guinea pigs (data not shown), which are functionally more mature than rats at equivalent postnatal ages.

DISCUSSION

The presence of dendritic spikes was initially inferred from fast prepotentials seen during intrasomatic current clamp recordings of hippocampal pyramidal neurons *in vivo* (19). Direct dendritic recordings *in vitro* (3–5) later confirmed the capacity of dendritic membranes to generate the underlying Na^+-mediated spikes, as well as Ca^{2+}-mediated spikes. By contrast, Purkinje cell dendrites generate only Ca^{2+}-dependent spikes (2), emphasizing a probable diversity in the electrical properties of dendritic membranes in different classes of neurons. In neocortical neurons, regenerative dendritic events have been inferred from extracellularly recorded action potentials that propagate from deep to superficial layers (20) and from fast small potentials seen in current clamp recordings (7, 8, 10, 21), but the site of origin of these events is uncertain; possible contamination by electrode-induced membrane damage, "double" impalements (22), or even electrotonically coupled neurons (9) make these data hard to interpret. The results of our experiments now provide direct evidence that, in neocortical pyramidal neurons, there are voltage-dependent Na^+ conductances present in dendritic membranes up to at least 80 μm from the soma and further suggest that regional Na^+ channel density may be similar over somata and proximal dendrites. However, there may be highly localized hot spots with higher Na^+ channel activity (see below). It should also be noted that our data were obtained largely from primary apical dendritic membrane—almost all of the secondary and tertiary dendrites had either been amputated by the dissociation procedure or had not yet developed in these immature neurons.

Recordings from immature feline cortical neurons have suggested that partial spikes, interpreted as originating in dendrites, are more frequent than in mature cortical cells (7, 8). Although, we cannot eliminate the possibility that dendritic Na^+ conductances are prominent in our experiments because neurons were obtained from young animals, the presence of relatively uniform Na^+ channel density over soma-dendritic membranes of cells obtained at P2–P6 at least suggests that ontogenetic change in Na^+ channel *distribution* is not prominent within this age range.† The importance of dendritic excitability in mature neurons is emphasized by a recent *in vivo* study of fast pyramidal tract cells in cats that suggests that fast dendritic action potentials can be activated in a significant proportion of neurons (ref. 21, but see ref. 8). Similar dendritic spikes are seen in neurons of both the hippocampus (19) and thalamus (23) of adult animals.

In spite of the existence of dendritic Na^+ channels, the actual capacity of dendritic membranes to generate spike activity in cortical neurons may be difficult to assess. Phasic or tonic dendritic inhibitory postsynaptic potentials might function to suppress dendritic electrogenesis, as occurs in hippocampus (5, 24). Also, the soma-proximal dendritic region, from which we have recorded Na^+ channel activity, may be electrotonically so compact that it behaves as one compartment in terms of Na^+ spike generation. This situation would make it difficult to dissociate dendritic and somatic components of full size Na^+-mediated action potentials in current clamp recordings but would not reduce the importance of dendritic excitability in enhancing the coupling of dendritic excitatory postsynaptic potentials to somatic activation.

Since dendritic and axonal amputations have occurred in our dissociated neurons, a redistribution of Na^+ channels onto dendrites, similar to that shown in axotomized vagal neurons (17), might be proposed to explain these results. It is well known that axotomy can affect Na^+-dependent action

†Other data show that there is a progressive increase in the *density* of Na^+ currents in pyramidal neurons from embryonic day 16 to P19 (14).

potentials, perhaps by altering the density and/or distribution of voltage-dependent Na^+ channels (25–30); however, it seems unlikely that such effects have influenced the outcome of the present experiments. All reports of probable dendritic spike generation in axotomized cells *in vivo* suggest that a period of from days to weeks is required before the phenomenon can be seen (25, 26). In our experiments dendritic Na^+ currents were recorded as early as 60 min after the dissociation procedure; this seems like an insufficient time for new Na^+ channel protein to be synthesized and transported to dendritic membrane. Although little is known about the rate of synthesis and turnover of Na^+ channels in cortical neurons, in neuroblastoma cells it is estimated that <3% of total channels are replaced per hour (31). If this finding is applicable to neocortical neurons, typically <10% of the channels present would be due to newly inserted membrane channel proteins in our experiments. Furthermore, as in skeletal muscle fibers (32), neuronal Na^+ channels are thought to be essentially immobilized in the membrane by intracellular elements (refs. 33–35, but see ref. 36). Unless the anchoring mechanism was disrupted by the dissociation, somatic channels would not be expected to have sufficient lateral mobility to move through the membrane to the dendrites. The existence of dendritic hot spots indicates that the structural elements that anchor Na^+ channels in the membrane are maintained to some extent in dissociated neurons.

Several functions for dendritic Na^+ spikes in neocortical neurons might be proposed (for reviews, see refs. 37 and 38). Previous studies using current source density analysis in both hippocampal CA_1 pyramidal neurons (39, 40) and dentate gyrus granule cells (41) indicate that orthodromic stimulation can activate an inward current "sink," which moves from the cell body layer into the dendritic region. The Na^+-dependent nature of this potential has been shown by its TTX sensitivity. The functional consequences of this soma–dendritic propagation could be activation of other dendritic voltage-dependent conductances. For example, propagation of a Na^+ spike into the dendrites could serve as a means for activation of high-threshold dendritic Ca^{2+} conductances (42) and consequent increases in intracellular Ca^{2+} that can have potentially important modulatory influences on neuronal excitability (43, 44).

A second important consequence of dendritic Na^+ conductances would be to generate booster potentials or fast prepotentials that would make distal synaptic potentials more likely to depolarize the soma and axon hillock area to initiate an axonal spike, as first proposed by Spencer and Kandel (19) for hippocampal pyramidal neurons. In support of this idea, extracellular and intradendritic recordings from these neurons reveal that, with stimulation intensities above threshold, it is possible to initiate a TTX-sensitive spike response in the dendrites, which then actively propagates to the somatic region (45). Whether dendritic Na^+-mediated spikes have a similar function in neocortical neurons depends on the density and distribution of the Na^+ channels (and other ionic conductances) on the distal dendritic tree. Dendritic hot spots (16, 17) containing higher densities of Na^+ channels (Fig. 3*B*, location 4) would be sites where the safety factor for coupling excitatory postsynaptic potentials to spike activation would be much greater, ensuring priority of these synapses in generating cell output. The high (40%) incidence of dendritic spikes evoked in fast pyramidal tract neurons by thalamic stimulation (21) might thus be a mechanism for assuring a high probability of information transfer from important thalamocortical afferents. This function of dendritic Na^+ channels (i.e., maintenance of an adequate safety factor in the extensive distal dendritic trees of cortical neurons) would of course be modulated by local membrane interactions with excitatory and inhibitory postsynaptic potentials and other voltage-dependent conductances (16, 46).

We thank Hilarey Feeser and Jay Kadis for technical support and R. K. S. Wong for helpful discussions regarding the dissociation technique. This work was supported by National Institutes of Health Grants NS06477 and NS12151 and the Morris and Pimly Research Funds.

1. Grundfest, H. (1959) in *Handbook of Physiology, Section 1: Neurophysiology*, eds. Field, J., Magoun, H. W. & Hall, V. E. (Am. Physiol. Soc., Washington, DC), Vol. 1, pp. 147–197.
2. Llinás, R. & Sugimori, M. (1980) *J. Physiol. (London)* **305**, 197–213.
3. Wong, R. K. S., Prince, D. A. & Basbaum, A. I. (1979) *Proc. Natl. Acad. Sci. USA* **76**, 986–990.
4. Benardo, L., Masukawa, L. & Prince, D. A. (1982) *J. Neurosci.* **2**, 1614–1622.
5. Masukawa, L. & Prince, D. A. (1984) *J. Neurosci.* **4**, 217–227.
6. Barrett, J. N. (1975) *Fed. Proc. Fed. Am. Soc. Exp. Biol.* **34**, 1398–1407.
7. Purpura, D. P., McMurtry, J. G., Leonard, C. F. & Malliani, A. (1966) *J. Neurophysiol.* **29**, 954–979.
8. Purpura, D. P. & Shofer, R. J. (1964) *J. Neurophysiol.* **27**, 117–132.
9. MacVicar, B. A. & Dudek, F. E. (1981) *Science* **213**, 782–785.
10. Woody, C. D., Gruen, E. & McCarley, K. (1984) *J. Neurophysiol.* **51**, 925–938.
11. Numann, R. E. & Wong, R. K. S. (1984) *Neurosci. Lett.* **47**, 289–294.
12. Kay, A. R. & Wong, R. K. S. (1986) *J. Neurosci. Methods* **16**, 227–238.
13. Hamill, O. P., Marty, A., Neher, E., Sakmann, B. & Sigworth, F. J. (1981) *Pflügers Arch.* **391**, 85–100.
14. Huguenard, J. R., Hamill, O. P. & Prince, D. A. (1988) *J. Neurophysiol.* **59**, 778–795.
15. Bezanilla, F. & Armstrong, C. M. (1977) *J. Gen. Physiol.* **70**, 549–566.
16. Traub, R. D. & Llinás, R. (1979) *J. Neurophysiol.* **42**, 476–496.
17. Sernagor, E., Yarom, Y. & Werman, R. (1986) *Proc. Natl. Acad. Sci. USA* **83**, 7966–7970.
18. Nowycky, M. C., Fox, A. P. & Tsien, R. W. (1985) *Nature (London)* **316**, 440–443.
19. Spencer, W. A. & Kandel, E. R. (1961) *J. Neurophysiol.* **24**, 272–285.
20. Spear, P. J. (1972) *Exp. Neurol.* **35**, 111–121.
21. Deschênes, M. (1981) *Exp. Brain Res.* **43**, 304–308.
22. Alger, B. E., McCarren, M. & Fisher, R. S. (1983) *Brain Res.* **270**, 137–141.
23. Maekawa, K. & Purpura, D. P. (1967) *J. Neurophysiol.* **30**, 360–381.
24. Wong, R. K. S. & Prince, D. A. (1979) *Science* **204**, 1228–1231.
25. Eccles, J. C., Libet, B. & Young, R. R. (1958) *J. Physiol. (London)* **143**, 11–49.
26. Kuno, M. & Llinás, R. (1970) *J. Physiol. (London)* **210**, 807–821.
27. Pitman, R. M., Tweedle, C. D. & Cohen, M. J. (1972) *Science* **178**, 507–509.
28. Goodman, C. S. & Heitler, W. J. (1979) *J. Exp. Biol.* **83**, 95–121.
29. Titmus, M. J. & Faber, D. S. (1986) *J. Neurophysiol.* **55**, 1440–1454.
30. Brismar, T. & Gilly, W. F. (1987) *Proc. Natl. Acad. Sci. USA* **84**, 1459–1463.
31. Waechter, C. J., Schmidt, J. W. & Catterall, W. A. (1983) *J. Biol. Chem.* **258**, 5117–5123.
32. Weiss, R. E., Roberts, W. M., Stühmer, W. & Almers, W. (1986) *J. Gen. Physiol.* **87**, 955–983.
33. Almers, W. & Stirling, C. (1984) *J. Membr. Biol.* **77**, 169–186.
34. Wollner, D. A. & Catterall, W. A. (1986) *Proc. Natl. Acad. Sci. USA* **83**, 8424–8428.
35. Catterall, W. A. (1981) *J. Neurosci.* **1**, 777–783.
36. Angelides, K. J., Elmer, L. W., Loftus, D. & Elson, E. (1988) *J. Cell Biol.* **106**, 1911–1925.
37. Llinás, R. (1975) *Adv. Neurol.* **12**, 1–13.
38. Purpura, D. P. (1967) in *The Neurosciences*, eds. Quarton, G. C., Melnechuk, T. & Schmitt, F. O. (Rockefeller Univ. Press, New York), pp. 372–393.
39. Miyakawa, H. & Kato, H. (1986) *Brain Res.* **399**, 303–309.
40. Richardson, T. L., Turner, R. W. & Miller, J. J. (1987) *J. Neurophysiol.* **58**, 981–996.
41. Jefferys, J. G. (1979) *J. Physiol. (London)* **289**, 375–388.
42. Grace, A. A. & Bunney, B. S. (1983) *Neuroscience* **10**, 317–331.
43. Alkon, D. L. & Rasmussen, H. (1988) *Science* **239**, 998–1005.
44. Gamble, E. & Koch, C. (1987) *Science* **236**, 1311–1315.
45. Turner, R. W., Meyers, D. E. R. & Barker, J. L. (1988) *Neurosci. Abstr.* **14**, 836.
46. Moore, J. W., Stockbridge, N. & Westerfield, M. (1983) *J. Physiol. (London)* **336**, 301–311.